14TH CANADIAN MASONRY SYMPOSIUM
MONTREAL, CANADA
MAY 16TH – MAY 20TH, 2021

COMPRESSIVE STRESS-STRAIN BEHAVIOUR OF UNREINFORCED MASONRY BOUNDARY ELEMENT PRISMS CONSTRUCTED WITH C-SHAPED BLOCKS

Zorainy, Mohamed[1]; Ashour, Ahmed[2]; Ala' T. Obaidat[3] and Galal, Khaled[4]

ABSTRACT

Reinforced masonry shear walls (RMSW) with masonry boundary elements (MBE) are rectangular walls with integrated MBEs at the wall extremities. The compressive stress-strain behaviour of the MBE prisms built using C-shaped blocks (C-MBEPs) varies from that of regular stretcher prisms due to the continuity of the grout core and the higher grout-to-shell area ratio. Few studies have investigated the stress-strain behaviour of MBEs built using C-shaped blocks. This study evaluates the compressive stress-strain behaviour of half-scale fully grouted C-MBEP and its constituents (i.e., masonry shell and grout core). In total, 8 fully grouted masonry prisms, 6 un-grouted masonry shells, and 18 grout cores were tested under concentric displacement-controlled compression loading. The test matrix is composed of two aspect ratios: two and five, and normal and high grout strengths. In addition, the effect of grout core treatment, i.e., air and wet treatment, was examined. Similar to masonry prisms made from stretcher blocks, the superposition of the load-displacement relationship of the grout core and the masonry shell was found not comparable to that of the grouted C-MBEP Prisms built with similar grout and masonry blocks.

KEYWORDS: *C-shaped blocks, grout, height-to-thickness ratio, masonry boundary element, stress-strain behaviour, superposition*

[1] Former M.A.Sc. Student, Department of Building, Civil and Environmental Engineering, Concordia University, 1515 St. Catherine West, Montreal, QC, Canada. Currently, Assistant Lecturer in the Department of Civil Engineering, Ain Shams University, Cairo, Egypt, mohamed.yosry@eng.asu.edu.eg

[2] Assistant Professor, Department of Structural Engineering, Cairo University, Cairo University Rd, 12613, Egypt, dr.ashour.ahmed@gmail.com

[3] Former PhD graduate, Department of Building, Civil and Environmental Engineering, Concordia University, 1515 St. Catherine West, Montreal, QC, Canada. Currently, Assistant Professor in the Faculty of Engineering, Philadelphia University, Jordan, aobaidat@philadelphia.edu.jo

[4] Professor, Department of Building, Civil and Environmental Engineering, Concordia University, 1515 St. Catherine West, Montreal, QC, Canada, khaled.galal@concordia.ca

INTRODUCTION

Reinforced concrete block masonry is widely used in the construction of low-rise residential and commercial buildings, especially in North America, as reinforced masonry seismic force resisting systems (SFRS) have proven their efficiency in resisting seismic loads. Recent studies [1-4] have shown an enhancement in wall ductility by introducing an integrated boundary element at the reinforced masonry shear wall (RMSW) ends. Masonry boundary elements (MBEs) allow the introduction of two layers of vertical steel rebars and, consequently, confining the wall's most stressed zone (under lateral loads) by means of hoop reinforcement.

Few studies have focused on the compressive stress-strain behaviour of reinforced MBEs. Abo El Ezz et al. [5] investigated the effect of increasing the confinement ratio on the post-peak behaviour and the strain ductility of MBEs constructed utilizing concrete stretcher blocks. They found that more strain ductility is achieved by decreasing the hoop spacing. However, utilizing stretcher blocks to build the MBEs imposed some limitations on the hoop spacing. Obaidat et al. [6] tested full-scale reinforced MBEs constructed by C-shaped blocks. Obaidat et al. [7] further investigated the effect of changing the hoop spacing, the longitudinal reinforcement ratio, and the grout strength on the axial stress-strain behaviour of half-scaled C-shaped reinforced MBEs. Obaidat et al. concluded that increasing the longitudinal reinforcement ratio, increasing the grout strength, and decreasing the hoop spacing all enhanced the peak and post-peak stress-strain performance [7]. Nonetheless, the compressive stress-strain behaviour of the unreinforced MBEs constructed using the C-shaped blocks has yet to be presented.

The main objective of this study is to investigate some of the main factors affecting the interaction between the shell and the grout core of unreinforced masonry boundary element prisms constructed with C-shaped blocks (C-MBEPs). The factors studied are the prism's aspect ratio, grout strength and the treatment of the grout samples. To achieve this objective, three types of specimens were constructed and tested (Figure 1). The first type was grouted C-MBEPs, where the prisms were grouted with normal and high strength grouts and had 2 height/thickness ratios (h/t), namely, 2 and 5. The second type was the C-MBEP shells (un-grouted masonry prisms of the same h/t ratios as the grouted C-MBEPs). The third type of specimens was grout prisms that replicated the grouted cores of the C-MBEPs. These grout prisms were cast from the same normal and high strength grouts used for the C-MBEPs and had the same dimensions as the cores of these prisms. The grout strength, treatment and aspect ratio effects were evaluated by observing the experimental results of the tested grout core prisms. Then, the superposition of the load-displacement behaviours of the shells and the grout cores were compared to the load-displacement behaviours of the corresponding C-MBEPs and discussed considering the studied factors.

EXPERIMENTAL WORK

Test Matrix

As illustrated in Figure 1, the test matrix of the current study consists of three groups: (1) fully-grouted MBE prisms, (2) un-grouted MBE shells, and (3) C-MBE grout core prisms (denoted in

Table 1 by BE, SH and GC, respectively). Three sets of MBE prisms constructed using C-shaped concrete masonry blocks were tested under concentric compression loading up to failure. As listed in Table 1, the first set, BE-N-2, had a height-to-thickness ratio, h/t, equal to 2 (four-courses) and built using normal-strength grout (i.e., noted by "N"). The other two sets, BE-N-5 and BE-H-5, had a height-to-thickness ratio equal to 5 (ten-courses) and were grouted using normal and high-strength grout (i.e., noted by "H"), respectively. In addition to the fully grouted MBE prisms, two sets of un-grouted MBE shells were constructed and tested under a similar loading procedure. The two ungrouted sets (i.e., noted by "0"), SH-0-2 and SH-0-5, had h/t equal to 2 and 5, respectively.

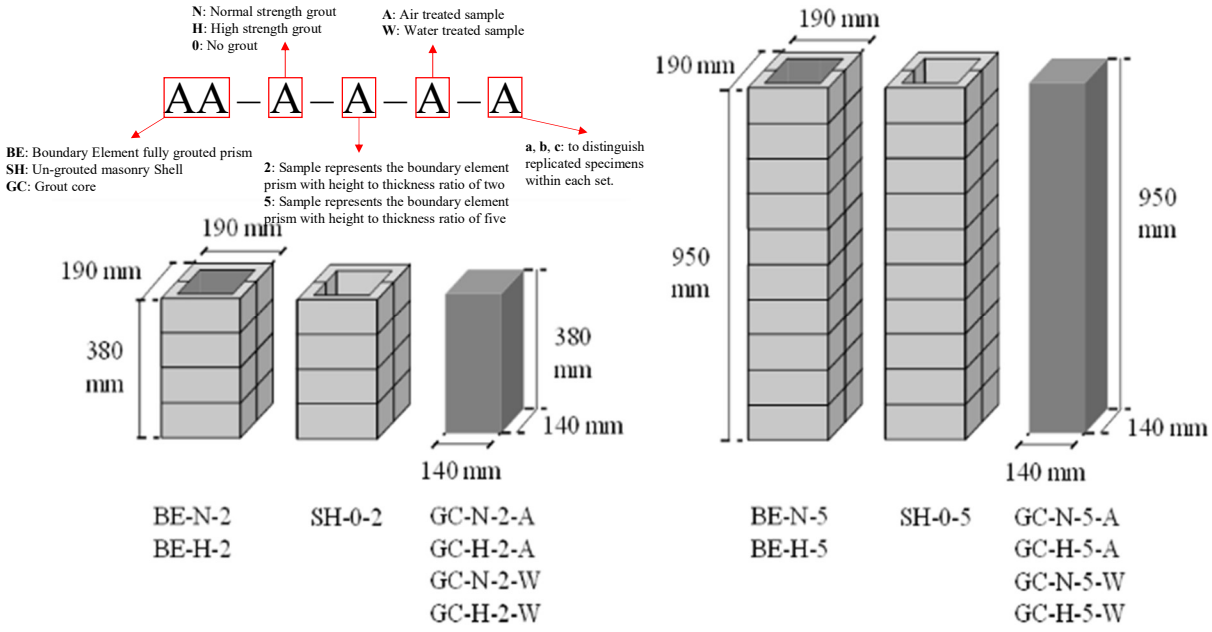

Figure 1: Schematic Drawings of the Tested Specimens with h/t = 2.0 and h/t = 5.0

Table 1: Experimental Test Matrix for MBE Prisms C-MBEP, Un-grouted Masonry Prisms (Masonry Shells), and Grout Core Specimens

ID	Grout Strength	Height-to-Thickness ratio	Actual Height-to-Thickness ratio	Curing	Number of specimens
BE-N-2	Normal	2	2	N/A	2
BE-N-5	Normal	5	5		3
BE-H-5	High	5	5		3
SH-0-2	N/A	2	2		3
SH-0-5		5	5		3
GC-N-2-A	Normal	2	2.7	Air	3
GC-N-5-A		5	6.8		1
GC-H-2-A	High	2	2.7		3
GC-H-5-A		5	6.8		1
GC-N-2-W	Normal	2	2.7	Water	3
GC-N-5-W		5	6.8		1
GC-H-2-W	High	2	2.7		3
GC-H-5-W		5	6.8		3

Moreover, eight sets of grout prisms, mimicking the grout cores inside the MBE prisms, were cast and tested under concentric compression loading. Each grout core had a square cross-section of side length equal to 140 mm and a height of 380 mm or 950 mm (Figure 1). These dimensions replicate the dimensions of the grout cores corresponding to the tested C-MBEPs. All the grout cores were constructed by casting the grout following the ASTM C1019 [8] standard. The blocks were laid so that they could act as molds for the grout cores. The inner faces of each space, specified for casting a grout specimen, were lined with paper towels as specified in ASTM C1019 [8]. The paper towels act as a permeable surface that allows the absorption of water from the grout core by the surrounding blocks while preventing bond between them.

Four pairs of grout cores were constructed with h/t equal to 2.7 and 6.8 representing the grout cores in C-MBEPs with h/t equal to 2 and 5, respectively (Table 1). For each h/t, two sets were cast using normal and high-strength grout. To investigate the effect of curing, following the construction, one set of grout cores was cured in water (i.e., 24 hours after pouring the grout) and the other set was air cured in their molds. Both sets were removed from the molds 24 hours before testing.

Material Properties

Half-scaled blocks were used in this experimental work due to the limited capacity of the available testing frame. The C-shaped blocks were tested for compressive strength according to the requirements of CSA A165 [9] and ASTM C140 [10] [11]. Five coupon specimens of dimensions 100 mm (length) x 50 mm (height) x 25 mm (thickness) were cut and were tested for compressive strength in the same direction of the actual loading (results in Table 2).

Table 2: Materials' Properties

Item	Batch #	Ultimate Load (kN)	Compressive Strength (MPa)	C.V.	Number of Specimens
Block	-	55.0	22.0	13.80%	10
Mortar	-	32.3	12.9	7.94%	12
Grout (NS)	Batch 1[a]	117.0	14.9	8.70%	3
	Batch 2[b]	122.5	15.6	4.34%	6
Grout (HS)	Batch 1[a]	353.0	45.0	4.75%	3
	Batch 2[b]	361.1	46.0	6.41%	6

[a]Batch 1 used for fully-grouted boundary element prisms.

[b]Batch 2 used for grout core specimens.

Prebagged type S mortar was used for joining the C-shaped block units in the shells and the grouted C-MBEPs. The mortar joints' thicknesses were approximately 5 mm each. The compressive strength of the mortar was evaluated according to CSA A179 [12]. Six 50 mm mortar cubes were tested for compressive strength for each mortar batch (results in Table 2).

Three cylinders (100-mm diameter and 200-mm height) were sampled from each grout batch. The grout was tested for compressive strength according to CSA A179 [12]. All the cylinders were cured in water before testing. The grout cylinders were capped by high-strength gypsum as

specified by ASTM C617 [13]. Due to the large number of samples, two grout batches were used (results in Table 2). High slump grout was used to avoid gaps or voids in the grouted core. The prisms were filled by grout in three layers with thorough compaction for each layer.

The testing was carried out under displacement-controlled loading. A rate of 0.005 mm/sec was utilized, up to a 0.002 axial strain. After that, a slower rate of 0.001 mm/sec was applied to capture the post-peak behaviour. The change in displacement was measured by linear variable differential transformers (LVDTs). Two LVDTs were positioned opposite to one another. The gauge length was half the height of the cylinder (100 mm). The gauge lines were parallel to the axis of the cylinder and centered about its mid-height, following the requirements of ASTM C469 [14]. The peak stress for the normal-strength grout occurred at a strain of 0.002, while the peak stress for the high-strength grout occurred at a strain of 0.0028. The initial stiffness for the normal and high strength grouts were 7.52 and 18.71 GPa, respectively.

Test Setup, Instrumentation, and Loading Protocol

All specimens were tested in a servo-controlled 2000 kN reaction frame under quasi-static concentric compression loading up to failure. High-strength gypsum was used between the upper and lower steel plates and the sample to ensure sample leveling and to prevent any voids between the specimen and the loading plates. The plates' dimensions and material followed the requirements of CSA S304 [15]. The verticality of the specimens was verified by two laser aligning devices positioned in two perpendicular directions. A spherical head was placed between the top of the specimen and the loading cylinder. The spherical head was checked before each test to ensure that it was free to tilt in any direction and that it was centered with the upper plate and the sample. At least four LVDTs were used to measure the displacement across the full height of all the specimens. The LVDTs were positioned so that there was one LVDT centered on each side of the tested prism (Figure 2). A rate of 0.005 mm/sec was utilized during testing, up to a 0.002 axial strain. A slower rate of 0.001 mm/sec was then applied to capture the post-peak behaviour.

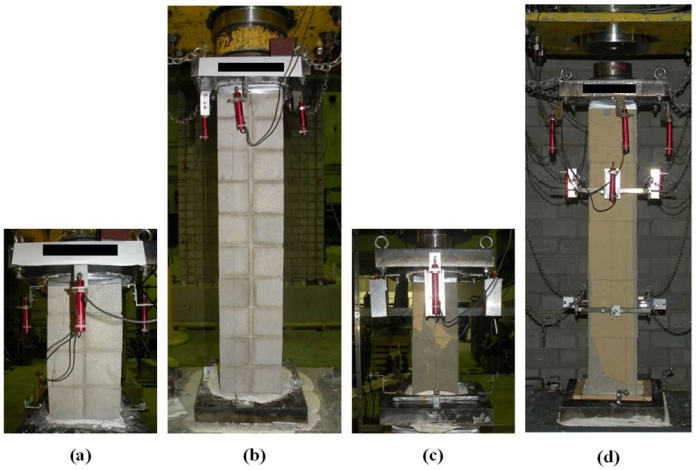

Figure 2: Test setup and instrumentation for masonry prisms with h/t ratios of: (a) two and (b) five, and grout cores representing the grout in BE prisms with height to thickness ratios of: (c) two and (d) five

RESULTS AND OBSERVATIONS

Fully-Grouted Boundary Elements Prisms

For C-MBEPs of h/t = 2.0 (BE-N-2), a shear mode conical shaped failure pattern was observed. On the other hand, a splitting failure was observed for the C-MBEPs with h/t = 5.0 (BE-N-5 and BE-H-5). The splitting failure started with vertical cracks in the vertical joints after reaching the maximum load, followed by partial spalling of the C-shaped units initiated by the expansion of the grout core. For all specimens, no buckling was observed during testing until their failure. The final failure mode consisted of vertical splitting cracks along the four sides, with the sides containing the vertical mortar joints having bigger and longer cracks, accompanied by partial spalling of the blocks and the crushing of the grout core (Figure 3).

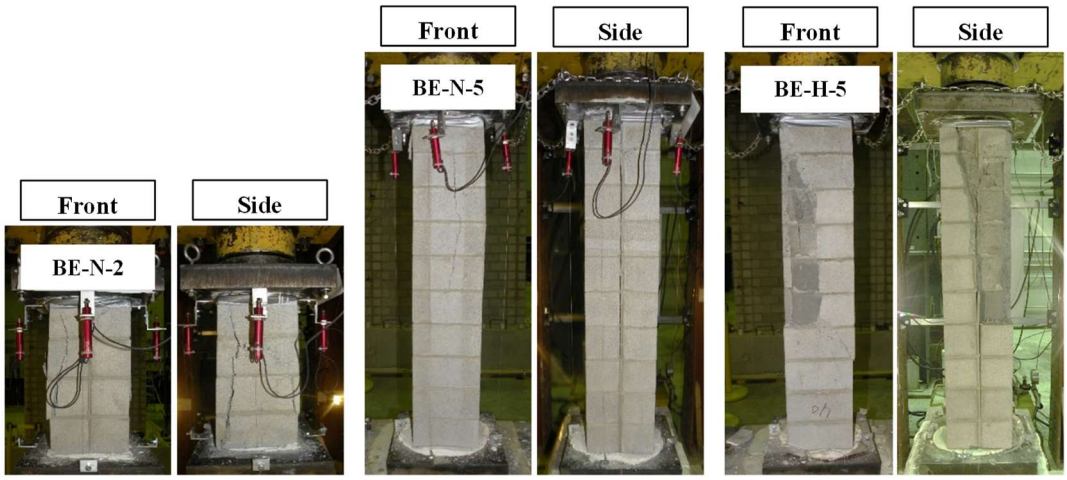

Figure 3: Observed failure patterns for fully-grouted Prisms BE-N-2, BE-N-5 and BE-H-5

Figure 4 shows the stress-strain behaviour of the individual specimens tested, along with the average behaviour for each category of prisms. The average behaviour was calculated by averaging the stresses at each strain level for all the specimens in each category. It is worth mentioning that these stresses are the average stresses observed against the strains measured by the four LVDTs on the four sides of each specimen at each strain level. The stresses were calculated based on the gross area of the specimen (i.e., 190 mm x 190 mm = 36100 mm^2). It should be noted that in Figure 4 sample BE-N-5-c is coincident with the average curve. Also, at high strain value the average is average curve is dominated by BE-N-5-a & c as BE-N-5-b failed at lower strain.

The results of testing the C-MBEPs are summarized in Table 3. Comparing the C-MBEPs grouted with the same normal strength grout (BE-N-2 and BE-N-5), it can be observed that h/t has considerable effect on peak stress but does not affect the peak strain. The average peak stress of the prisms with h/t = 2 (BE-N-2) is 1.2 times that of the prisms with h/t = 5 (BE-N-5). Considering the failure patterns, the prisms of different heights show different peak stresses due to the confining effect of the loading machine end platens. The constraining effect of the platens on the top and

bottom of the prisms alters the compressive stress-strain behaviour of the prisms, leading to two distinctive failure modes, peak stress values, and elastic moduli for the prisms of h/t = 2.0 and 5.0.

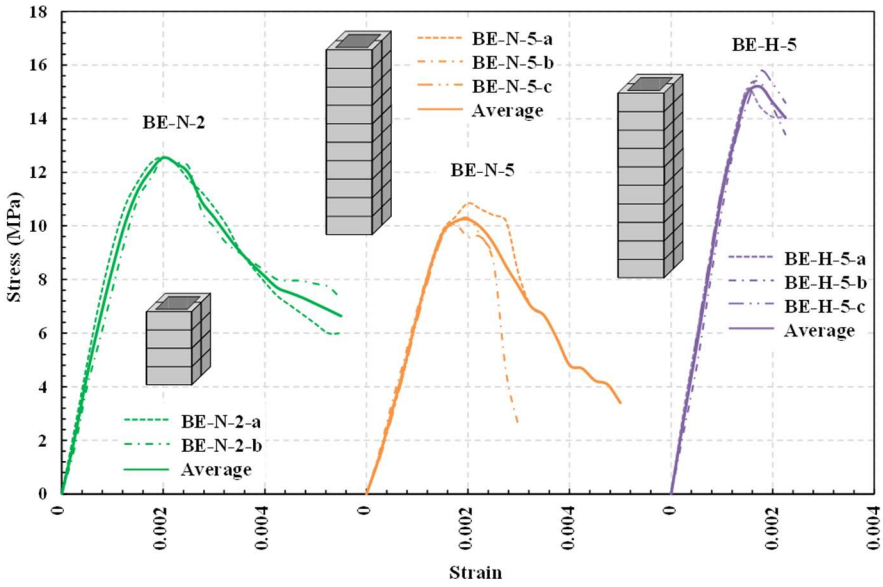

Figure 4: Stress-strain Curves for Masonry Boundary Element Prisms C-MBEPs

Table 3: Results of Tested Masonry Boundary Elements Prisms C-MBEP, Un-grouted Masonry Prisms (Shells), and Grout Core Specimens

ID	Ultimate Load (kN)	Strength (MPa)	C.V.	Strain at Peak	C.V.	Elastic Modulus (GPa)	C.V.
BE-N-2	457.0	12.66	0.28%	0.0020	2.83%	8.88	14.14%
BE-N-5	380.5	10.54	2.83%	0.0019	9.03%	6.15	9.22%
BE-H-5	563.2	15.60	2.43%	0.0016	6.31%	10.98	12.03%
SH-0-2	214.5	13.0	1.90%	0.0021	8.31%	9.42	12.43%
SH-0-5	171.1	10.37	1.09%	0.0018	7.95%	8.32	1.92%
GC-N-2-A	402.8	20.55	13.61%	0.0034	5.81%	8.97	9.04%
GC-N-5-A	392.0	20.00	N/A	0.0025	N/A	10.65	N/A
GC-H-2-A	1018.8	51.98	2.76%	0.0043	3.97%	19.42	9.15%
GC-H-5-A	948.1	48.37	N/A	0.0034	N/A	22.28	N/A
GC-N-2-W	405.0	20.66	1.63%	0.0030	17.69%	11.27	11.79%
GC-N-5-W	437.1	22.30	N/A	0.0028	N/A	8.37	N/A
GC-H-2-W	996.7	50.85	2.17%	0.0041	8.16%	17.96	17.59%
GC-H-5-W	935.1	47.71	12.28%	0.0026	15.31%	26.44	10.54%

The effect of increasing the grout strength can be observed by comparing BE-H-5 to BE-N-5. Tripling the grout core compressive strength from 14.9 MPa to 45 MPa increased the MBE's peak stress by only 50%. Increasing the grout strength also led to a stiffer prism by increasing the elastic modulus by almost 1.8 times (from 6.15 GPa to 10.98 GPa). However, this increase in stiffness had a slight effect on peak strain.

Un-Grouted Boundary Element Shells

As shown in Figure 5, a shear mode conical shaped failure pattern was observed for the masonry shells with h/t = 2.0 (SH-2) and h/t = 5.0 (SH-5). This failure pattern is similar to the common pattern observed in ungrouted masonry prisms and wallets [16], [17]. For all specimens, no buckling was observed during testing until the sudden failure.

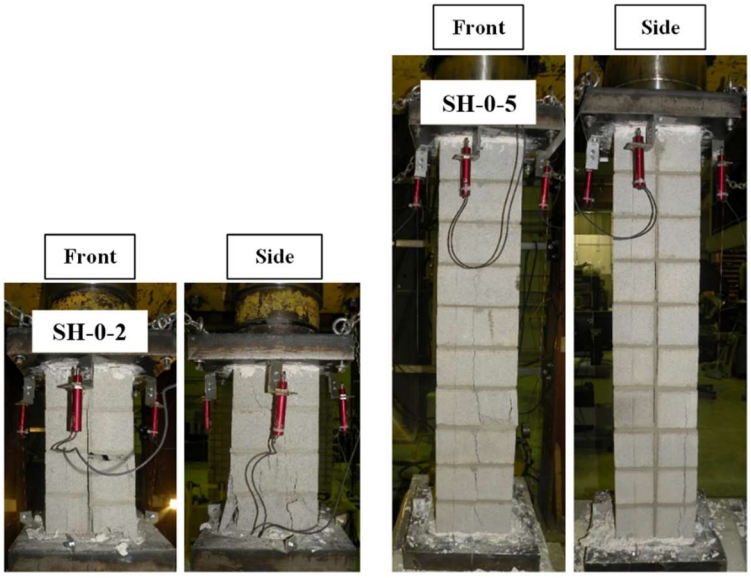

Figure 5: Observed failure patterns for the un-grouted BE shells SH-0-2 and SH-0-5

The stress-strain behaviours for the un-grouted MBE shells are illustrated in Figure 6. The stress-strain behaviours of the individual specimens in each category as well as the average behaviour were calculated similar to the procedure adopted for the fully grouted MBE prisms. However, the area used was the net area of the prisms (190 mm × 190 mm – 140 mm × 140 mm = 16500 mm^2).

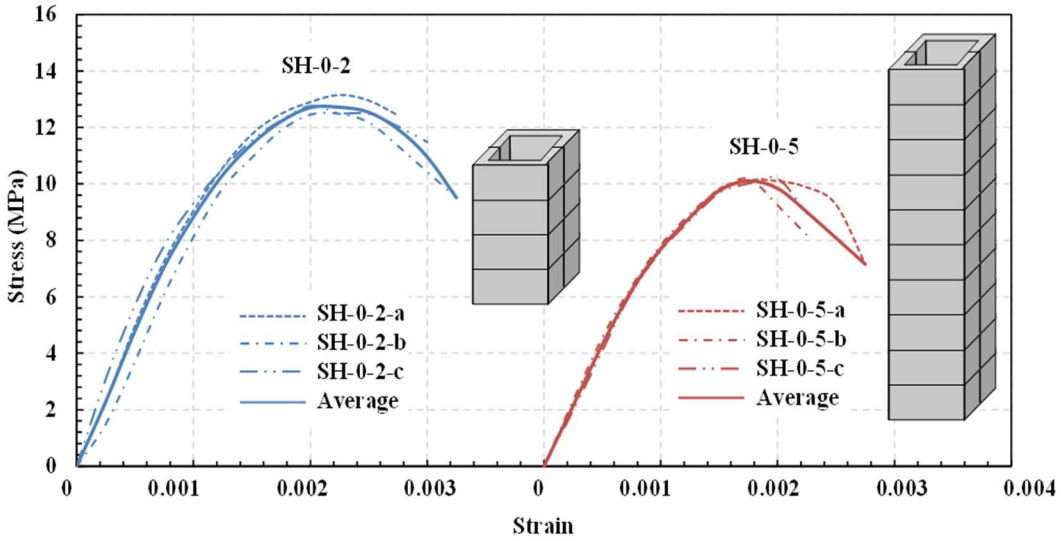

Figure 6: Stress-strain Curves of Un-grouted Masonry Shells

The results of testing the un-grouted MBE shells are summarized in Table 3. Similar to the results of the grouted prisms, the platen effect was evident in the behaviour and results of the ungrouted prisms. The average peak stress for the prisms of h/t = 2.0 is 1.25 times that of the prisms of h/t = 5.0. The average peak strains for both prism sets are around 0.002. The ratio of 1.25 is also comparable to the 1.2 corresponding to the grouted prisms. It can be concluded that shells and grouted prisms of h/t = 2.0 and 5.0 are affected by the platen confinement in the same manner.

Grout Cores

The stress-strain behaviours of the grout core prisms are presented in Figure 7. This figure shows the stress, computed as the measured load divided by the core area (i.e., 19600 mm^2), against the average longitudinal strains (i.e., the average of the four LVDTs readings). None of the grout cores showed any visible cracking before failure. The specimens resisted the loads applied while being intact until the brittle failure, which was more intense in the high-strength grout specimens. The results of testing the grout cores are summarized in Table 3.

DISCUSSION

Treatment Effect

The effect of treatment can be observed by comparing the results of air-treated and wet-treated grout core prisms presented in Table 3.

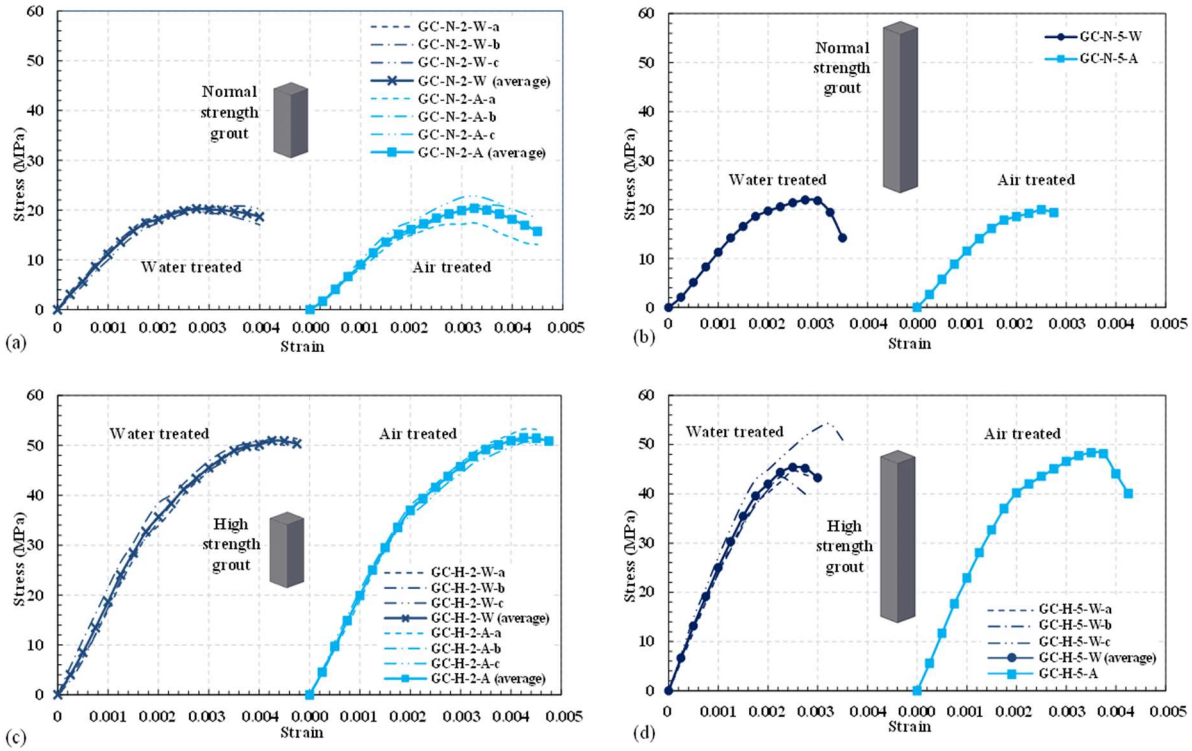

Figure 7: Stress-strain Curves for Normal Strength Grout Cores Representing the Cores of MBE Prisms with h/t of: (a) Two and (b) Five, and High Strength Grout Cores Representing the Cores of MBE Prisms with h/t of: (c) Two and (d) Five

In general, no significant difference was found between grout specimens cured in water and those left to cure between the blocks. This was true for normal and high strength grouts and for specimens of h/t equals to 2.0 and 5.0. Moreover, Figure 7 shows that the effect of treatment on the stress-strain of the grout core prisms is also insignificant. This can be explained in light of the assumption presented in Sturgeon et al. [18], which states that the surrounding blocks retain the mixing water for the grout cores. That assumption is supported by the observation that after the failure of the cores in this study, the core specimens were found to be moist on the inside.

Aspect Ratio Effect

C-MBEPs of h/t = 2 grouted with normal-strength grout showed a 20% increase in strength compared to prisms of h/t = 5, while shells of h/t = 2 showed a 25% increase in strength compared to cores with h/t = 5. Increasing the h/t from 2.0 to 5.0 for air-treated normal strength grout core prisms decreased the strength by 3%, while for wet-treated grout core prisms the effect was an 8% increase in strength. As for high-strength grout core prisms, changing the h/t from to 2.0 to 5.0 decreased the strength by 7% for air-treated and wet-treated specimens. The correction factor for masonry block prisms of h/t = 2.0 in CSA S304 [15] is set to 0.85 to mitigate the platen effect. This value indicates a strength increase of 15% for these prisms compared to prisms of h/t = 5.0. The results of the grout core prisms show percentages that are lower than the CSA value.

The platen effect on the peak stress is less obvious in the grout cores than in the shells and grouted prisms. This is attributed to the actual h/t of the shorter grout core prisms being close to 3.0. This h/t, combined with a length-to-thickness ratio of 1.0, results in peak stresses that are approximately equal to these of the longer prisms [19].

Superposition of Masonry Shell and Grout Core Load-Displacement Curves Versus that of the Tested Boundary Elements

The load-displacement behaviour of the MBE prisms is compared against the load-displacement behaviour of the corresponding shells and air-treated grout cores in Figure 8. As shown in this figure, for various displacement levels, the load resisted by the C-MBE shell is added to the corresponding grout core load to result in the superposition curve, which is compared to the observed C-MBEP experimental load-displacement curve. The first clear observation is that for samples with h/t = 5, the load resisted by the grout core only is higher than that resisted by the corresponding prism. This can be observed by comparing the grout core ultimate load to the C-MBEP ultimate load in Table 3, even without adding any contribution from the masonry shell. This observation is even clearer in high-strength samples where GC-H-5-A and GC-H-5-W resisted almost 400 kN more load than BE-H-5, i.e., 70% more than the prism's capacity. It can also be observed from Figure 8 that the prism peak strength is achieved at a strain comparable to the masonry shell peak strain, similar to what was observed by Priestley and Hon [20].

For the MBE prisms of normal strength grout and h/t = 2, there is a good agreement between the superposition behaviour and the tested prism behaviour, nearly until the cracking of the shell. After that, the superposition overestimates the resistance of the prism with the increase in axial

displacement. In other words, the superposition fails to detect the post-peak phase of the prism's load-displacement behaviour. For the MBE prisms of normal strength grout and h/t = 5, the superposition tends to overestimate the load capacity of the prism at any displacement. The overestimated load value (superposition load – tested load) tends to increase with the increase of the displacement. Also, the superposition fails to capture the post-peak behaviour of the prism. For the MBE prisms with high strength grout and h/t = 5, the superposition again tends to overestimate the load capacity at any displacement. This overestimation of load value increases with the increase of the displacement. The superposition's failure at capturing the post-peak behaviour of the prism is still visible.

Figure 8 clearly shows that the grout strength decreases when incorporated in a masonry prism. However, this study did not capture the main contributing factor behind this strength reduction. Further work is needed to compute the contribution of different factors (e.g., the shrinkage effect on the grout strength, water absorption from grout core by the shell, and the strain difference between the grout and the masonry shell) on the grout strength within a fully grouted prism [21].

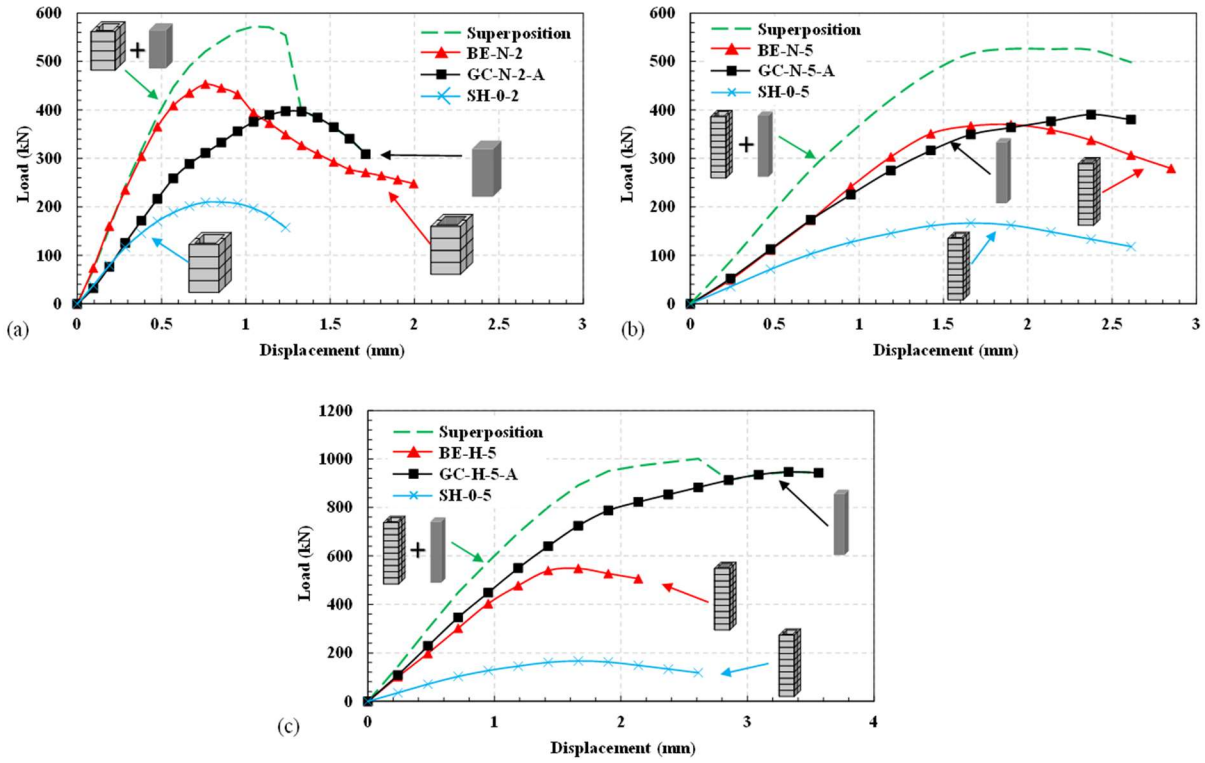

Figure 8: Comparison of the Load-displacement Relationships of Un-grouted MBE Prisms, Grout Cores, and their Superposition with: (a) C-MBEPs having h/t = 2 and Constructed Using Normal Strength Grout, (b) C-MBEPs having h/t = 5 and Constructed Using Normal Strength Grout, (c) C-MBEPs having h/t = 5 and Constructed Using High Strength Grout

A recent study by AbdelRahman and Galal [22] studied the effect of scaling and grout shrinkage on the response of unreinforced MBEs. It was concluded that wetting un-grouted masonry prisms

just before grouting has a significant effect on C-MBE prism compressive strength and post peak behaviour. Wetted C-MBE masonry prisms compressive stress-strain behaviour demonstrated excellent agreement when compared to the superposition of masonry shell and grout core.

CONCLUSIONS

Improving the compressive stress-strain behaviour of unreinforced MBE concrete prisms has a direct impact on the performance of Reinforced Masonry Shear Walls (RMSWs) with MBEs. Understanding and improving the interaction between the grouted core and the outer shell is the cornerstone of enhancing unreinforced masonry performance. In this study, the compressive stress-strain behaviour of half-scale fully-grouted C-shaped MBEPs and their constituents (i.e., masonry shell and grout core) are studied. In total, 8 fully-grouted masonry prisms, 6 un-grouted masonry shells, and 18 grout cores were tested under concentric compression loading up to failure. The matrix includes two prisms' aspect ratios, two and five, and two grout strengths, normal (15 MPa) and high (45 MPa) strength. The effects of the grout height-to-thickness ratio and grout treatment (air and wet) on the stress-strain behaviour of the grout samples were also examined.

Based on this experimental work, it can be concluded that the grout treatment has a negligible effect on the stress-strain behaviour. The average difference in the peak stress between the air- and wet-treated grout cores was 5% for the normal strength grout. This difference was even lower in high-strength grout specimens. It was observed that as the aspect ratio decrease the compressive strength increase (20% on average). This observation is valid for grouted masonry prisms, un-grouted masonry prisms (masonry shell) and normal strength grout prisms (grout core). As for high-strength grout core prisms, changing the h/t from 2.0 to 5.0 decreased the strength by 7%.

Superposition of the strengths of the masonry shell and the grout core based on their respective areas overestimates the strength of the C-MBEPs. More specifically, it overestimates the load capacity at any displacement value along the load-displacement curve of the prisms grouted with normal or high-strength grouts.

This study opens the door for future work in this field to enhance the compressive strength of masonry assemblages and walls.

ACKNOWLEDGEMENTS

The authors acknowledge the support for this work from the Natural Sciences and Engineering Research Council of Canada (NSERC), l'Association des Entrepreneurs en Maçonnerie du Québec (AEMQ), the Canadian Concrete Masonry Producers Association (CCMPA) and the Canada Masonry Design Centre (CMDC).

REFERENCES

[1] Shedid, M. T.; El-Dakhakhni, W. W. and Drysdale, R. G. (2010). "Alternative Strategies to Enhance the Seismic Performance of Reinforced Concrete-Block Shear Wall Systems." *J. Struct. Eng.*, 136(6), 676-689.

[2] Banting, B. R. and El-Dakhakhni, W. W. (2012). "Force- and displacement-based seismic performance parameters for reinforced masonry structural walls with boundary elements." *J. Struct. Eng.*, 138(12), 1477-1491.
[3] Ezzeldin, M.; El-Dakhakhni, W. and Wiebe, L. (2017). "Experimental Assessment of the System-Level Seismic Performance of an Asymmetrical Reinforced Concrete Block–Wall Building with Boundary Elements." *J. Struct. Eng.*, 143(8), 04017063.
[4] Albutainy, M.; Ashour, A. and Galal, K. (2017). "Effect of Boundary Elements Confinement Level on The Behaviour of Reinforced Masonry Structural Walls with Boundary Elements." *Proc., 13th Canadian Masonry Symposium*, Halifax, NS, Canada.
[5] Abo El Ezz, A.; Seif Eldin, H. M. and Galal, K. (2015). "Influence of confinement reinforcement on the compression stress-strain of grouted reinforced concrete block masonry boundary elements." *Structures*, 2, 32-43.
[6] Obaidat, A. T.; Abo El Ezz, A. and Galal, K. (2017). "Compression behavior of confined concrete masonry boundary elements." *Eng. Struct.*, 132, 562-575.
[7] Obaidat, A. T.; Ashour, A. and Galal, K. (2018). "Stress-strain behavior of C-shaped confined concrete masonry boundary elements of reinforced masonry shear walls." *J. Struct. Eng.*, 144(8), 04018119.
[8] ASTM C1019 (2014). "Standard Test Method for Sampling and Testing Grout." *ASTM International*, West Conshohocken, PA, USA.
[9] CSA A165 (2014). "CSA Standards on concrete masonry units." *CSA Group*, Toronto, ON, Canada.
[10] ASTM C140 (2015). "Standard Test Methods for Sampling and Testing Concrete Masonry Units and Related Units." *ASTM International*, West Conshohocken, PA, USA.
[11] Zorainy, M. Y.; Ashour, A. and Galal, K. (2018). "Comparing Canadian and American Standards Requirements for Evaluating Masonry Compressive Strength." *Proc., 15th International Conference on Structural and Geotechnical Engineering*, Cairo, Egypt.
[12] CSA A179 (2014). "Mortar and grout for unit masonry." *CSA Group*, Toronto, ON, Canada.
[13] ASTM C617 (2015). "Standard Practice for Capping Cylindrical Concrete Specimens." *ASTM International*, West Conshohocken, PA, USA.
[14] ASTM C469 (2014). "Standard Test Method for Static Modulus of Elasticity and Poisson's Ratio of Concrete in Compression." *ASTM International*, West Conshohocken, PA, USA.
[15] CSA S304 (2014). "Design of masonry structures." *CSA Group*, Toronto, ON, Canada.
[16] Barbosa, C. S.; Lourenço, P. B. and Hanai, J. B. (2010). "On the compressive strength prediction for concrete masonry prisms." *Mater. Struct. Constr.*, 43(3), 331-344.
[17] Zhou, Q.; Wang, F.; Zhu, F. and Yang, X. (2017). "Stress–strain model for hollow concrete block masonry under uniaxial compression." *Mater. Struct. Constr.*, 50(2), 1-12.
[18] Sturgeon, G. R.; Longworth, J. and Warwaruk, J. (1980). "An Investigation of Reinforced Concrete Block Masonry Columns." *Structural Engineering Report No. 91*, University of Alberta, Edmonton, AB, Canada.
[19] Hassanli, R.; ElGawady, M. A. and Mills, J. E. (2015). "Effect of dimensions on the compressive strength of concrete masonry prisms." *Adv. Civ. Eng. Mater.*, 4(1), 175-201.
[20] Priestley, M. J. N. and Hon, C. Y. (1984). "Prediction of Masonry Compression Strength Part:1." *New Zeal. Concr. Constr.*, 28, 11-14.
[21] Zorainy, M. Y. (2019). "Compressive Stress-strain of Unreinforced Masonry Boundary Element Prisms." *MSc thesis*, Concordia University, Montreal, QC, Canada.
[22] AbdelRahman, B. and Galal, K. (2020). "Influence of pre-wetting, non-shrink grout, and scaling on the compressive strength of grouted concrete masonry prisms." *Constr. Build. Mater.*, 241, 117985.